

Plasmon induced quantified agglomeration of SiO₂ nanoparticles to improve in efficiency in solar cell

P. Sarkar^{a,*}, S. Panda^b, B. Maji^a, A. K. Mukhopadhyay^c

^aDepartment of ECE, National Institute of Technology, Durgapur- 713209, India

^bDr. Sudhir Chandra Sur Institute of Technology & Sports Complex, Kolkata-700074, India

^cMargadarshak (Mentor), AICTE, New Delhi -110070, India

The impact of plasmonic confinement induced by the SiO₂ nanosphere utilized as a photonic absorber in a solar cell is investigated in this paper. The modified Stober technique is utilized for irradiation experiments using the size and shape of colloidal silica nanoparticles at two dosages of 0.485mg/ml and 0.693mg/ml solutions. The agglomerated silica is placed as an absorbent layer on a solar cell, and the J-V characteristics are studied under solar irradiation. The enhancement in efficiency and J_{sc} is far greater than predicted induced in photon injection caused by silica nanoparticle coating under coverage limit.

(Received August 9, 2022; Accepted November 2, 2022)

Keywords: Plasmon, Silica, Solar cell

1. Introduction

With increasing global energy demand and as well as environmental impact, renewable energy has become more in vogue than conventional fossil energy. Solar photovoltaic cells are more optimistic than other renewable sources due to their inherent properties. Recently research in this field has competed for more potential [1-2]. Silicon is commonly taken as a base material for solar cells. The conventional silicon solar cell is mostly fabricated at wafer thickness from 180 μm to 300 μm [3]. Due to low cost and reliable processing technologies, silicon, is still the preferred material for photovoltaic applications. Today almost about 95% of production is fabricated with crystalline silicon photovoltaic cell, and the rest 5% contributed to thin-film solar cells [3-4]. Comparable to other energy, the preferment is the cost of a solar cell to be reduced and the energy conversion efficiency improved. The use of TF silicon solar cell is another approach to adopt for this cost reduction due to the need for less material and so less processing energy. It requires the photonic absorption methodologies in thin film cell such as incident irradiance is scattered in various angles and that the photonic path length is increased optically in a thin-film layer. Traditional light tapping methods, like silicon surface texturing, may not, however, be suited as the surface roughness goes to several micrometers [2].

Plasmonics is an emerging field of nanotechnology that characterized by nanoparticles where photonic absorption is to scatter photons on nano-dimension to improve in absorption solar cell. In recent years, the field of plasmonics has expanded into the recent area of emerging materials and process methodology due to available of reliable synthesis and characterization processes for nanoparticles of desired dimensions, shapes, and surface distribution. [2, 5]. Many research groups have used various techniques to manufacture nanoparticles, such as films on chemical Synthesis, Electron beam lithography, metal island structure [6–10]. Figure 1 shows localize plasmon, SiO₂ nanoparticles on silicon cell and field propagation

* Corresponding author: parthasarkar.info@gmail.com
<https://doi.org/10.15251/JOR.2022.186.723>

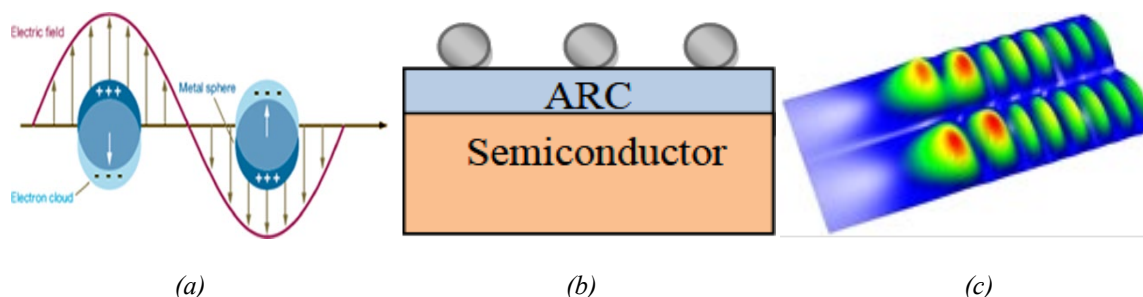


Fig. 1. (a) Localize plasmon due bounded electron cloud, (b) silica particle on ARC glass and silicon structure, (c) absorbed field propagation inside cell structure.

Surface plasmon excitation investigations have been recently carried out using metal nanoparticles to scatter incoming irradiance and direct it into a thick silicon layer [1, 2, 8-11]. At plasmon resonance, the scattering capacities of the nanoparticles become large and depend on the geometry of the nanoparticles, the particle distribution, composition, and their surroundings [5, 12-14]. The optimization of these attributes can, therefore, tune the resonance at surface plasmonic resonance (SPR) at particular wavelength. Titanium (Ti), aluminum (Al), copper (Cu), gold (Au), chromium (Cr), Silver (Ag) are preferred Drude metal that enable surface plasmon. Silver and gold, because of their inherent properties specifically in the visible spectrum, are widely used nanometals in surface plasmon [15-19].

It is relied on the use of metallic nanoparticles in photonic absorption on the front surface of photovoltaic cells, as scattering efficiency should be the lowest absorption loss at that spectral region. Any nanoparticles that absorb light will become lost in the spectrum and do not contribute to the device's photogeneration. However, nanoparticles are highly absorbed in dipolar resonance wavelengths, reducing the effect on improving light absorption in cell layer and hence reducing the overall positive impacts of the nanoparticles. [20]. This reduction is minimized when the size and shape are effectively improved to increase radiative efficiency, which is the ratio of scattering to photonic extinction [21].

A part of incident irradiance is scatter from the layer that causes a reflection from the surface of the medium, while an additional fraction is scattered in the substratum. The scattering efficiency and scattered fractions in the substratum cannot, however, be maximized independently, and the properties of the nanoparticles can be obtained in accordance with their acceptable values. Dielectric nanoparticle appears as suitable material since their absorption at optical wavelengths is negligible compared with metallic nanoparticles. The impact of silicon nanoparticles on the absorption and production of photovoltaic silicon has been investigated in the field of electromagnetic scattering. The impact of silica nanoparticles on the photonic absorption and generation of photocurrent in silicon solar cells has been investigated in the electromagnetic scattering field. Surface plasmon resonance (SPR) of metallic nanoparticles has shown itself to be responsible for plasmonic behavior [22-23]. However, the photonic absorption brings down cell efficiency while thin sensitized layer is used. This results in intensive research on such types of cells for improved device design to improve efficiency, leading to improvement in collection efficiency due to photonic absorption [24].

2. Experimental

A modified Stober approach was used to create the silica nanoparticles, which is one of the most popular techniques. This methodology generates spherical silica nanoparticles by hydrolyzing alkyl silicate and then condensation in alcoholic solutions using NH_3 as a catalyst. The solution of 85ml ethyl alcohol is dissolved in 14 ml of double-distilled water and stirred by a magnetic stirrer for 1hr at 31°C until silica nanoparticles with an average size of 200nm to 300nm

are obtained. The desired particle size distribution can be achieved by altering the starting solution material concentrations or modifying the alkyl and alcoholic groups.

Following that, a solution of 6 ml Tetra-Ethyl Ortho-Silicate (TEOS) with a concentration of 98% and 3 ml of NH₄OH with a concentration of 30% was added drop-wise to the solution to maintain the desired alkalinity. This aqueous solution is stirred for the next 1 hr at the stirring rate of 2000 rpm until the whole solution turns milky white. The solution was then centrifuged, and the isolated silica nanoparticles were rinsed three to four times in various alcoholic mediums. The separated particles are heated from 47°C to 52°C for four to five hours. Finally, the particles are subsequently placed under ultrasonic exposure in an ethanol medium to produce the final colloidal solution.

The prepared silica nanoparticles in ethanol are spin-coated on a bare Si surface with a speed of 200 rpm to obtain a uniform coating of silica nanoparticles on the silicon surface. The synthesized specimen was tested by UV-VIS spectrophotometer (Perkin Elmer Perkin Elmer Lamda 35 spectrophotometer) to measure the absorption band. X-ray diffraction spectrometer (Bruker AXS with X-ray source: Cu K) for diffraction pattern and Field Emission Scanning Electron Microscope (FESEM). The Reflection characteristics of the substrate, measured in Bentham PVE300. For the photo-catalytic experiment, the desired illumination at AM1.5 with 100mWcm⁻² irradiance is measured under 300-watt Xenon lamp. Figure 2 shows reflectance vs. irradiance wavelength for coating solutions with different doses in order to direct impact on coverage area.

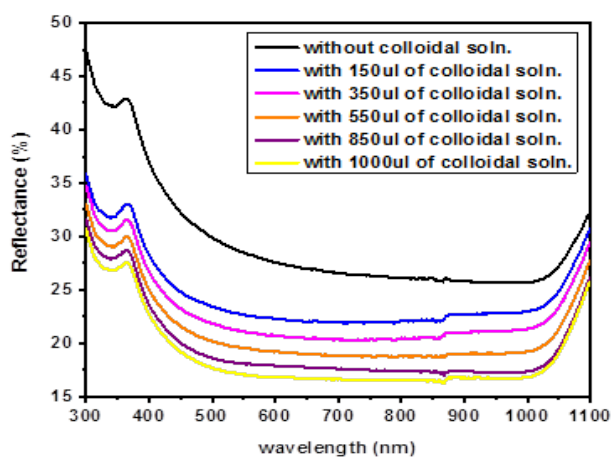


Fig. 2. Reflectance vs. wavelength with different dose (1st dose to 5th dose).

It is seen that at a given particle size the reflectance decreases with an increase of coverage (or dosage). After several observations with irradiated samples exhibit, the best possible improvement in reflection is achieved for a thin layer of coating at a speed of 480 rpm for 0.693mg/ml dosage.

3. Results and Discussion

The optical extinction behavior has an impact on the absorption and scattering phenomena. Backscattering is essentially loss, also known as reflectance, while front scattering can be additive depending on particle size, position, and local environment. The extinction is an addition to absorption and scattering taken as optical efficiency metric [25]. So, the optical scattering and extinction are calculated as

$$\sigma_{sca} = \frac{\lambda^2}{2\pi} \sum_{n=0}^{\infty} (2n+1) (|a_n|^2 + |b_n|^2)$$

$$\text{and } \sigma_{ext} = \frac{\lambda^2}{2\pi} \sum_{n=0}^{\infty} (2n+1) \text{Re}(a_n + b_n)$$

Under the solar irradiance absorption spectra, average particle sizes have been theoretically estimated by

$$R = \frac{\lambda}{\sqrt{2Q_{ext}}} \sqrt{\sum_{n=0}^{\infty} \{(2n+1) \text{Re}(a_n + b_n)\}}$$

where, λ is average wavelength of solar irradiance spectra, Q_{ext} is optical extinction efficiency, a_n and b_n are defined with Mie coefficients, which are characterized using Ricatti-Bessel functions, where n is an index ranging from 1 to ∞ [25-31]. Figure 3 shows FDTD simulation of localized plasmonic effect in solar cell with the presence of SiO₂ nanoparticle under normalized electric field.

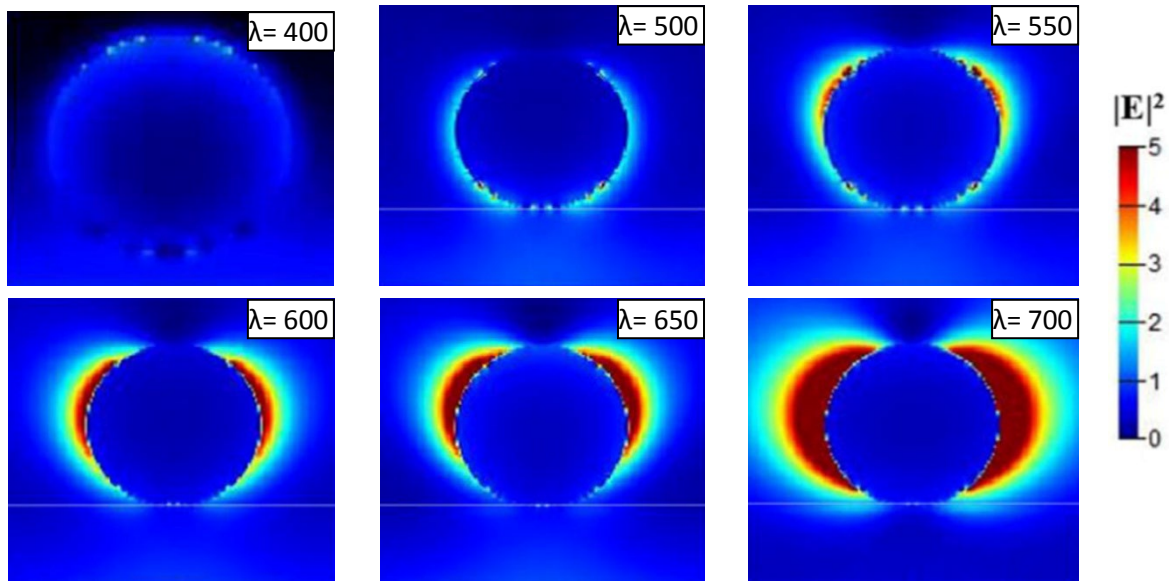


Fig. 3. FDTD simulation of normalized electric field on silica nanoparticales on silicon with localized plasmonic effect.

From FDTD simulations, it also exhibits plasmonic enhancement, including front scattering with scale down of irradiance spectra, which becomes progressive. The absorption spectra of irradiated samples clearly show improvement in their absorption edges as compared to the various doses of colloidal silica in figure 4.

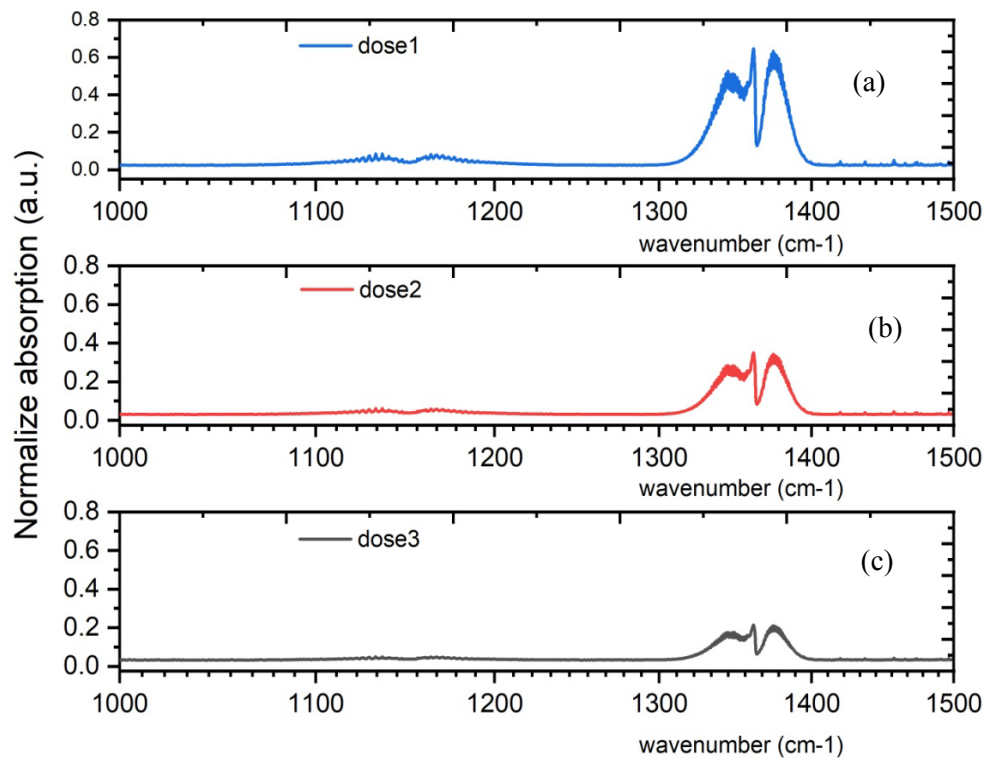


Fig. 4. UV-Visible absorption spectroscopy of various doses of silica coating solution with coverage density; (a) dose 1: 0.693mg/ml (b) dose 2: 0.485mg/ml (c) dose3: 1.027mg/ml.

From the Debye-Scherrer formula, the crystalline planes that correlate to the X-ray diffraction peaks are (101) and (110) under two thetas glancing angle is shown in figure5, the average silica nanoparticles size was approximated 175nm to 219nm for optimal dosage specimen.

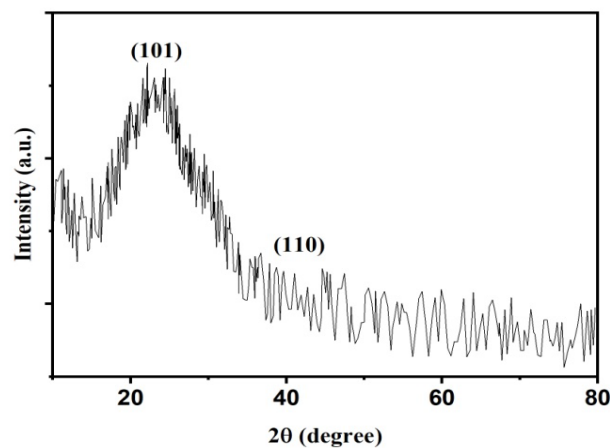


Fig. 5. XRD spectra of SiO_2 nanoparticlaes with dose1: 0.693mg/ml coating solution.

Figure 6 shows images of agglomerated size and shape of SiO_2 nanosphere taken with a Field Emission Scanning Electron Microscope(FESEM) with different dosages. FESEM image clearly shows that SiO_2 nanoparticles are round in shape, with diameters varying from 190nm to 300nm with different sample solutions.

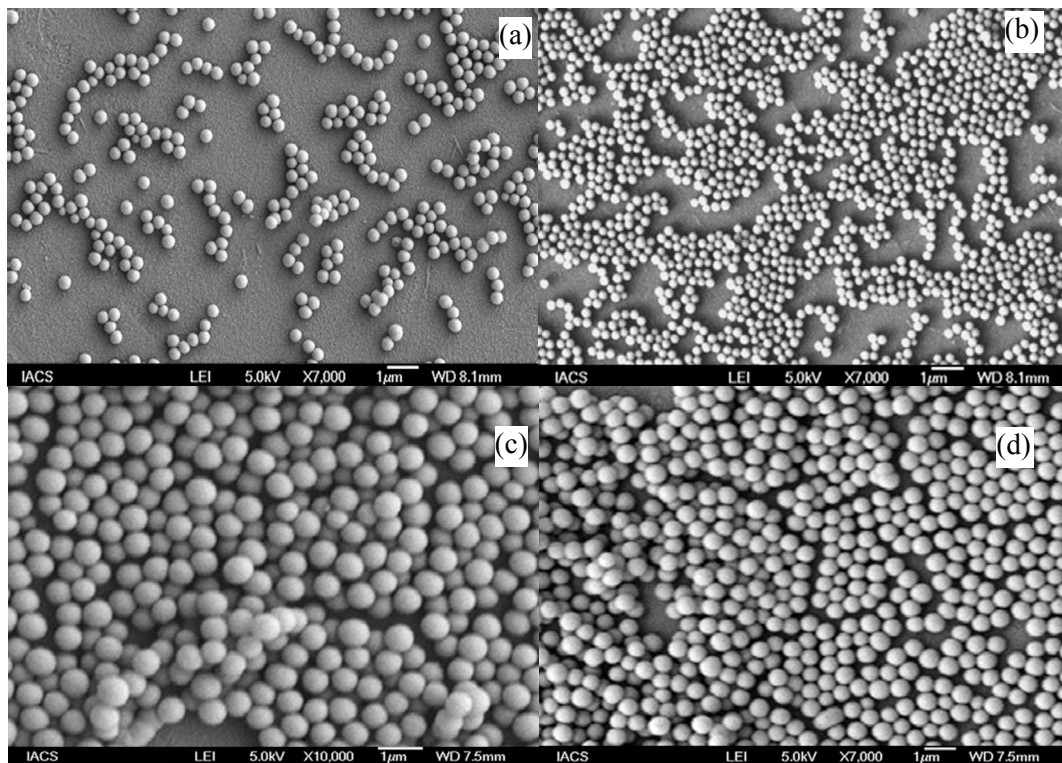


Fig. 6. FESEM image of SiO_2 dosages with Lower secondary electron detector (LEI) with GB (a) 0.365mg/ml solution at $\times 7000$ with working distance 8.1nm, (b) 0.693mg/ml solution at $\times 7000$ with working distance 8.1nm, (c) 0.485mg/ml solution $\times 10000$ with working distance 7.5nm (d) 1.027mg/ml solution at $\times 7000$ with working distance 7.5nm.

There are various fundamental parameters that can be employed to define solar cell efficiency. The electrical parameters like fill factor (FF), short-circuit current (J_{sc}) and open-circuit voltage (V_{oc}), etc., and are more accountable. At low voltages, the current density in an ideal solar cell is near to J_{sc} . When $J_{sc} = 0$ at the other end of the J-V curve as shown in figure 7, the cell dissipates its electrical power. The efficiency of solar cells is defined as

$$\eta = \frac{FF \cdot J_{sc} \cdot V_{oc}}{P_{in}}$$

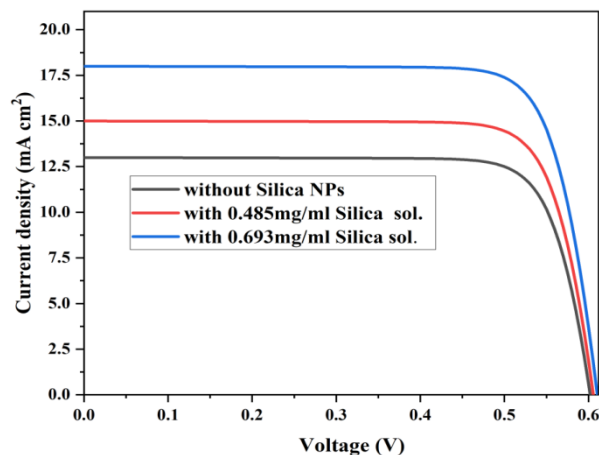


Fig. 7. J-V characteristic of SiO_2 nanoparticles based silicon solar cell (SSC) with various doses as sensitized absorber.

Table 1. Electrical parameters of various silica doses on silicon solar cell.

Samples	Concentration	J_{sc} (mA/cm ²)	V_{oc} (V)	Fill Factor (FF)	Efficiency ($\eta\%$)
Without SiO ₂	–	12.96	.601	0.8014	6.24
Dose 1_SiO ₂ Nps	0.693mg/ml sol.	17.89	.611	0.7954	8.69
Dose 2_SiO ₂ Nps	0.485mg/ml sol.	14.99	.610	0.7991	7.3

4. Conclusion

The improvement in efficiency and short circuit current density is substantially more than estimated from the increase in photon injection due to silica nanoparticles coating. The nanostructure and optical properties of specimen doses are illustrated using UV-Vis spectrograph, X-ray diffraction pattern, and FESEM to select the optimal solution of doses. This is due to enhanced plasmonic trapping induced by the bending of incoming light into large angles generated by repeated reflection from neighboring agglomerated SiO₂ nanosphere on the glass surface. At lower dosages of silica-induced photon ionic irradiation, the J-V characteristics reveal an increase in current density and efficiency than the reference sample. For sample doses, 0.485mg/ml and 0.693mg/ml coating solutions show improvement in efficiency at 1.06% and 2.45% with respect to bare sample. Subsequently, the cell's photoconversion efficiency decreases with increasing dosage.

References

- [1] V.E. Ferry, J.N. Munday, H. A. Atwater, *Adv Mater*, 22(43), 4794(2010); <https://doi.org/10.1002/adma.201000488>
- [2] H. Atwater, A. Polman, *Nature Materials* 9, 205 (2010); <https://doi.org/10.1038/nmat2629>
- [3] International Technology Roadmap for Photovoltaic (ITRPV), 11th edition, April (2020); <https://itrvp.vdma.org/en>
- [4] S. Philips, Fraunhofer Institute for Solar Energy Systems, ISE, Freiburg, Germany, (2019); <https://www.ise.fraunhofer.de/content/dam/ise/de/documents/publications/studies/Photovoltaics-Report.pdf>
- [5] J. Liu, H. He, D. Xiao, S. Yin, W. Ji, S. Jiang, D. Luo, B. Wang, Y. Liu, *Materials*, 11(10) 1833(2018); <https://doi.org/10.3390/ma11101833>
- [6] C.M. Cobby, S.E. Skrabalak, D.J. Campbell, *Plasmonics* 4, 171 (2009); <https://doi.org/10.1007/s11468-009-9088-0>
- [7] P. Colson, C. Henrist, R. Cloots, *J Nanomater* 2013, 948510 (2013); <https://doi.org/10.1155/2013/948510>
- [8] I. G. Gonzalez-Martinez, A. Bachmatiuk, V. Bezugly, J. Kunstmann, T. Gemming, Z. Liu, G. Cuniberti, M. H. Rummeli, *Nanoscale*, 8, 11340(2016); <https://doi.org/10.1039/C6NR01941B>
- [9] J. Krajczewski, K. K. Taj, A. Kudelsk, *RSC Adv.*, 7, 17559(2017); <https://doi.org/10.1039/C7RA01034F>
- [10] L. Yang, J. Wei, Z. Ma, P. Song, J. Ma, Y. Zhao, Z. Huang, M. Zhang, F. Yang, X. Wang, *Nanomaterials* (Basel, Switzerland), 9(12), 1789(2019); <https://doi.org/10.3390/nano9121789>
- [11] X. Chen, B. Jia, J.K. Saha, B. Cai, N. Stokes, Q. Qiao, Y. Wang, Z. Shi, M. Gu, *Nano Lett.*, 12(5), 2187(2012); <https://doi.org/10.1021/nl203463z>
- [12] J. Olson, S. Dominguez-Medina, A. Hoggard, L. Y. Wang, W. S. Chang, S. Link, *Chem. Soc. Rev.*, 44, 40(2015); <https://doi.org/10.1039/C4CS00131A>
- [13] A. Agrawal, I. Kriegel, D. J. Milliron, *J. Phys. Chem. C*, 119(11), 6227(2015);

<https://doi.org/10.1021/acs.jpcc.5b01648>

[14] M. Kim, J. H. Lee, J. M. Nam, *Adv. Sci.* 6, 1900471(2019);

<https://doi.org/10.1002/advs.201900471>

[15] P. West, S. Ishii, G. Naik, N. Emani, V. Shalaev, A. Boltasseva, *Laser & Photon. Rev.*, 4, 795(2010); <https://doi.org/10.1002/lpor.200900055>

[16] J. Jana, M. Ganguly, T. Pal, *RSC Adv.*, 6, 86174(2016);

<https://doi.org/10.1039/C6RA14173K>

[17] A. Derkachova, K. Kolwas, I. Demchenko, *Plasmonics*, 11, 941(2016);

<https://doi.org/10.1007/s11468-015-0128-7>

[18] M. Tzschoppe, C. Huck, J. Vogt, F. Neubrech, A. Pucci, *J. Phys. Chem. C*, 122(27), 15678 (2018); <https://doi.org/10.1021/acs.jpcc.8b04209>

[19] J. K. Bhattarai, M. H. U. Maruf, K. J. Stine, *Processes* 8(1), 115(2020);

<https://doi.org/10.3390/pr8010115>

[20] A. Yu, W. S. Akimov, S. Koh, Y. Sian, S. Ren, *Appl. Phys. Lett.* 96, 073111(2010);

<https://doi.org/10.1063/1.3315942>

[21] A. Yu, W. S. Akimov, S. Koh, K. Ostrikov, *Opt. Express* 17, 10195(2009);

<https://doi.org/10.1364/OE.17.010195>

[22] T. Hayakawa, S. T. Selvan, M. Nogami, *Appl. Phys. Lett.* 74, 1513 (1999);

<https://doi.org/10.1063/1.123600>

[23] O.L. Malta, P.A. Santa-Cruz, G.F. De Sá, F. Auzel, *J. of Luminescence*, 33(3),261(1985);

[https://doi.org/10.1016/0022-2313\(85\)90003-1](https://doi.org/10.1016/0022-2313(85)90003-1)

[24] C. M. Hsu, C. Battaglia, C. Pahud, Z. Ruan, F. J. Haug, S. Fan, C. Ballif, Y. Cui, *Adv. Energy Mater.*, 2, 628(2012); <https://doi.org/10.1002/aenm.201100514>

[25] P. Sarkar, S. Panda, B. Maji, A. Kr. Mukhopadhyay, *Int. J. of Nanoparticles*,10, 77(2018);

<https://doi.org/10.1504/IJNP.2018.092678>

[26] P. Sarkar, S. Panda, B. Maji, A. Kr. Mukhopadhyay, *Nanosci & Nano-Asia*,10(4), 425

(2020); <https://doi.org/10.2174/2210681209666190830100710>

[27] P. Sarkar, S. N. Surai, S. Panda, B. Maji, A. Kr. Mukhopadhyay, "Contemporary Advances in Innovative and Applicable Information Technology", AISC, Springer, Singapore,812,67 (2019);

https://doi.org/10.1007/978-981-13-1540-4_8

[28] P. Sarkar, A. Manna, S. Panda, B. Maji, A. Kr. Mukhopadhyay, *Materials Today:*

Proceedings, 5, 21225(2018); <https://doi.org/10.1016/j.matpr.2018.06.522>

[29] P. Sarkar, S. Panda, B. Maji, A. Kr. Mukhopadhyay, 2018 IEEE Electron Devices Kolkata Conference (EDKCON), 437(2018); <https://doi.org/10.1109/edkcon.2018.8770473>

[30] P. Sarkar, S. Panda, B. Maji, A. Kr. Mukhopadhyay, 2017 Devices for Integrated Circuit (DevIC), 175(2017); <https://ieeexplore.ieee.org/document/8073931>

[31] P. Sarkar, B. Maji, A. Manna, S. Panda, A.K. Mukhopadhyay, *Int. J. Nanosci.*,17(04), (2017);

<https://doi.org/10.1142/S0219581X17600286>